19th INTERNATIONAL CONGRESS ON ACOUSTICS
MADRID, 2-7 SEPTEMBER 2007

INVESTIGATING THE ROLE OF ULTRASONIC SCATTERING IN THE WAVE ABSORPTION PHENOMENON

PACS: Cs 43.35.Ud

Cortela, Guillermo[1], C. A. Pereira, Wagner[2]; San Emeterio, Jose Luis[3], Negreira, Carlos[1]
[1] Laboratorio de Acústica Ultrasonica, Igua 4225, Montevideo, Uruguay; gcortela@fisica.edu.uy
[2] Biomedical Engineering Program – COPPE/UFRJ, Rio de Janeiro, Brazil
[3] Instituto de Acústica - CSIC, Madrid, Spain

ABSTRACT
To calculate the thermal dose in therapeutic ultrasound only the absorption phenomenon is considered. Nevertheless scattering can be non negligible, thus influencing global attenuation and consequently the thermal dose. This work proposes an experimental approach of the role scattering has in temperature generated by therapeutic ultrasound in biological phantoms. These phantoms mimic the acoustical and thermal properties of biological tissues. This study was conducted with continuous wave ultrasound at 1 and 3 MHz and 2 W/cm^2. Five phantoms were used in the experiments. The first one composed of one single agar-gel based layer 85-mm thick. The others composed of two layers: one of 42-mm agar-gel and the other with 43-mm agar-gel mixed with graphite or PVC powder as scatterers. Seven thin thermocouples were inserted in the phantoms (two in the first layer and the others in the second one, 5 mm from each other) and connected to standard instrumentation. The phantoms were heated by ultrasound for 10 min. Preliminary results show that the layer with graphite powder reaches up to 4ºC more than the other phantoms at the same depth. Therefore, we have an initial indication how scattering can influence heating patterns and should be taken in consideration, at least in some scenarios.

INTRODUCTION
It is well known the ultrasonic energy absorption phenomenon by biological tissues. In fact this property is applied in therapeutic procedures [1-3]. In 1948, Pennes has established a relationship between ultrasound and temperature by proposing the so called Biothemic equation [4]. In this model, several biophysical concepts related to ultrasound (US) are included, like blood perfusion, metabolic sources of heat, thermal doses, etc. For therapeutic applications, the thermal dose (which means answering the question of how much intensity for how much time) is the critical issue and is usually determined from the global tissue attenuation. Usually the contribution of wave scattering is assumed as negligible [5]
Ultrasonic scattering is dependent on several parameters (US frequency, scatterers density, wavelength-to-scatter size relation, etc), including the distance travelled by the wave. In general, propagation of ultrasound in biological soft tissue is assumed to follow the Born Approximation. This work proposes a preliminary experimental investigation of the role of scattering in temperature generated by therapeutic ultrasound in biological phantoms.

Theory
The ultrasonic field generated by a plane circular transducer, in continuous mode excitation is given by the Rayleigh-Sommerfeld Integral:

$$p_m = \frac{ikr_{(\vec{r})}c_{s(\vec{r},T)}}{2p}\iint_{S_N} u_n \frac{\exp(-ikr_{mnq})}{r_{mnq}} dS_n \qquad (\text{Eq. 1})$$

where p_m is the acoustic pressure at the point (x_m, y_m, z_m), $r(\vec{r})$ the medium density, $c_s(\vec{r},T)$ the US velocity, k the real part of the wave number, u_n the excitation of the n-th point source, r_{mnq} the distance from point m to point q of the $n_{(x_{nq}, y_{nq}, z_{nq})}$ in the transducer surface and S_n is the area of the n-th element.

Biological tissues are absorbing media. The usual procedure to include attenuation in the model is to modify equation 1 by changing k in the exponential term to k_c, where $k_c=k-ia$ is the complex wave number and α the attenuation coefficient.

The interaction of the pressure filed with biological tissues generates a temperature field which can be modelled by the Biothermic equation as follows [3]:

$$r_t c_t \frac{\partial T}{\partial t} = \nabla \cdot (k_t \nabla T) + r_b c_b w_b (T - T_a) + Q(\vec{r}) \qquad (\text{Eq. 2})$$

where T is temperature in time t and at point (x,y,z), r_t is medium density, c_t medium specific heat, k_t medium conductivity, w_b blood perfusion rate, r_b blood density, c_b blood specific heat, T_a arterial-blood temperature and $Q(x,y,z)$ acoustic power per unitary volume.

The first right-side term of equation (2) describes the heat diffusion process; the second term is related to cooling due to blood perfusion. The third term describes the thermal field due to the attenuation of the ultrasonic energy and is given by the following equation.

$$Q(\vec{r}) = a(\vec{r},T)\frac{|p_m(\vec{r})|^2}{rc_s} \qquad (\text{Eq. 3})$$

where $a(\vec{r},T)$ is the attenuation coefficient as a function of position and temperature, and rc_s is the medium acoustic impedance. One can obtain an estimate of the temperature rise that may occur in tissue due to the attenuation of an ultrasonic beam by assuming that attenuation is entirely due to absorption [6]

$$Q(\vec{r}) = m_a(\vec{r},T)\frac{|p_m(\vec{r})|^2}{rc_s} \qquad (\text{Eq. 3'})$$

where $m_a(\vec{r},T)$ is the absorption coefficient as a function of position and temperature [7-9]. Several works indicate that temperature field is influenced by several parameters [10, 11], but, when considering long heating times, as in US therapy, blood perfusion is the most important one.

When an ultrasonic wave travels through a scattering medium part of it forms a coherent wave as result of the ensemble of all possible scatterer configurations. This coherent wave preserves initial propagation direction and presents an exponential decay as a function of depth that can be described by the mean elastic free path (ℓ_S). The other part of the original wave contributes to incoherent propagation [12, 13].
The single scattering theory is characterized by the exponential decrease of the coherent intensity I_C [14-16], according to:

$$I_C = I_0 T_C(z) = I_0 e^{-z f s_T} \qquad (\text{Eq. 4})$$

where T_C is the amplitude transmission coefficient, defined as the ratio between the spectra of the scattered and the emitted pulse, within the bandwidth of interest, I_C and I_0 are the coherent and incident intensity respectively, z the depth, ϕ the volume fraction (number of scatterers per volume unity) and σ_T the total scattering crossection. If a medium is composed of identical scatterers, the mean elastic freepath ℓ_S can be calculated from ϕ and σ_T of one scatterer as

$$\ell_S = \frac{1}{f s_T} \qquad (\text{Eq. 5})$$

By applying eq. (5) in (6), the coherent intensity can be written as

$$I_C = I_0 e^{-z/l_S} \qquad (\text{Eq. 6})$$

EXPERIMENTAL SETUP

The temperature signals were acquired according to the experimental setup in figure 1. A commercial physiotherapeutic US equipment (SONOPULSE – IBRAMED, Brazil), several phantoms, thermocouples and a multiplexer circuit connected to a PC.

Phantoms

Five phantoms were constructed that simulate the thermo-acoustic properties of soft biological tissues. One of them was a homogeneous layer entirely made of agar (no scattering material)

and is used as a reference. The other four phantoms have two layers. The first one was made of homogeneous agar. The second one was made of a mixture of agar with graphite (or PVC) powder to produce scattering. The powder volume fraction was kept constant in all cases. The scattering material properties are depicted in Table 1 and the phantoms layer thicknesses and compositions are shown in Table 2.

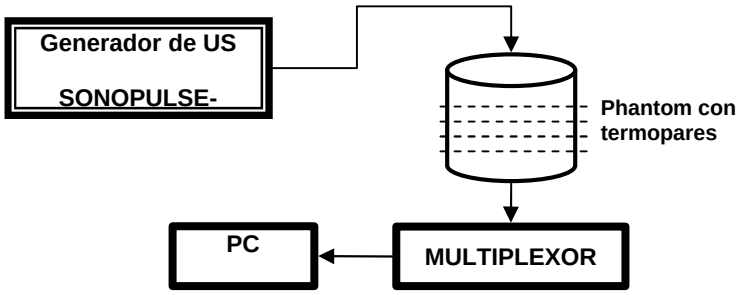

Figura 1. Experimental setup for temperature measurements.

Table 1. Scattering material properties for the phantoms to simulate different thermal and acoustic properties of biological tissues.

	ρ_t (kg/m^3)	Z (Mrayls)	c_t(J/gK)	k_t (W/mK)
PVC	1.38	1.38	1—1.5	0.12—0.25
Graphite	2.17	9.39	0.7	6

Table 2. Layer thicknesses and powder mass for each phantom.

	Phantom 1	Phantom 2	Phantom 3	Phantom 4	Phantom 5
Agar-agar	90 mm	47 mm	47 mm	47 mm	47 mm
PVC	--	--	--	43 mm/0.38g	43 mm/0.6g
Graphite	--	43 mm/0.38g	43 mm/0.6g	--	--

The mean freepath ℓ_s given by equation 5 depends only on ϕ for the same size and shape of the scattering element. Therefore we can relate the ℓ_s values of phantoms with different mass percentages of the same scatterer type as ℓ_{s1}=1.6 ℓ_{s2}, where the sub-index 1 and 2 refers to the mass quantities 0.38g y 0.6g respectively.

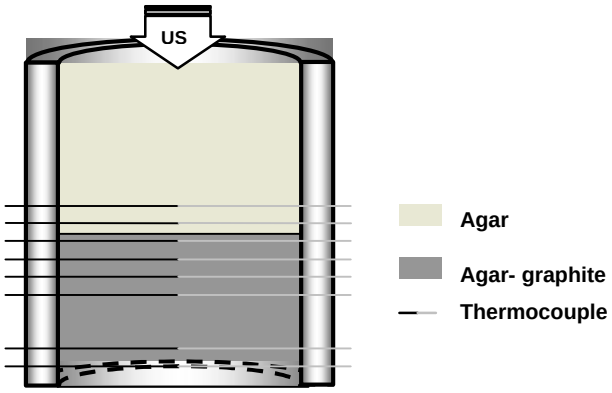

Figure 2. Phantom sagittal view including the thermocouple placements. The junctions are placed along the central axis of the cylinder which coincides with the piezoelement centre.

Thermocouples

The calibrated thermocouples are made of Constantan (Cu55/Ni45)-Chromel (Ni90/Cr10) junctions and present an average radio of 0.125 mm. They are located parallel to the face of the transducer as in figure 2.

Ultrasound

The US field is generated by the Ibramed equipment in continuous-mode and at 1 and 3 MHz. Insonification is kept for 10 minutes at 2.0 W/cm^2 intensity.

RESULTS AND DISCUSSION

The data acquisition was made by means of a multiplexer equipment connected to a PC. The temperature sampling frequency was 1 sample every 10 seconds. The obtained temperature curves are shown in fig. 3-5.

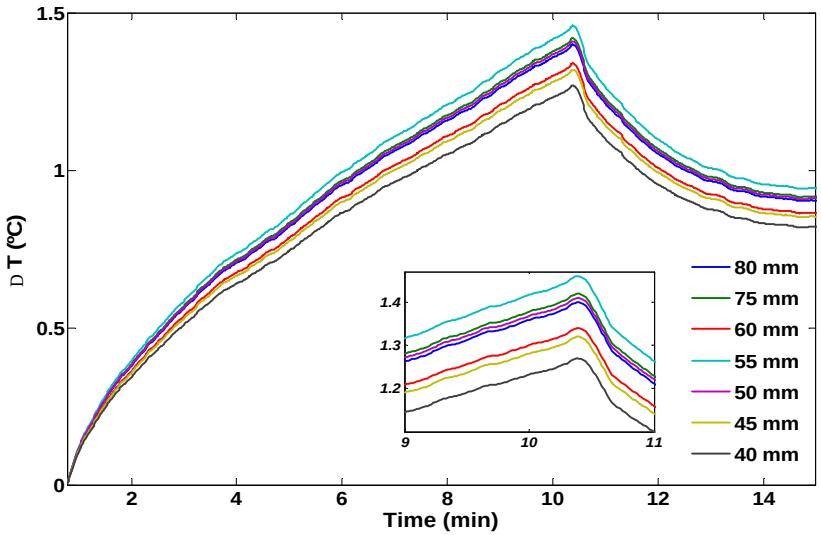

Figure 3. Temperature curves for each depth of Phantom 1 (homogeneous single-layered). Insonification in continuous mode at 2 W/cm^2) for a 10-minute period. Insonfication starts 30 seconds after the system is turned-on.

Table 3 summarizes maximum values of temperature increments after a 10-minute insonification (2.0 W/cm^2). One can see the ΔT values for the different depths in all 5 phantoms. The nearfield limit is ($d^2/4\lambda$) ≈60mm. Figures 4 and 5 show the temperature curves for the two-layered phantoms.

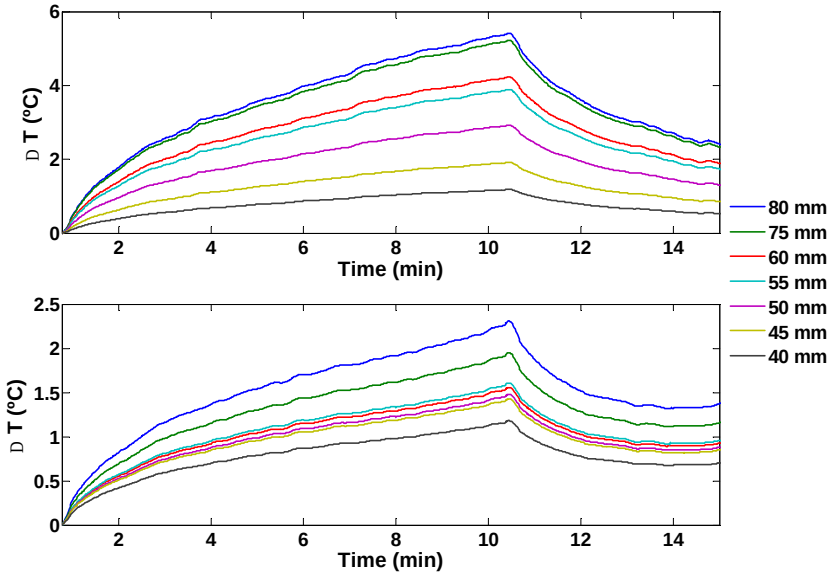

Figure 4. Temperature curves for phantom 3 (superior) and phantom 2 (inferior), insonified in continuous mode (2 W/cm^2) for 10 minutes.

On the other side it is possible to observe the effect of reflection in the two-layered phantoms 2 and 3 (one graphite layer). The ΔT for both phantoms at 45-mm depth (almost the same depth where the two-layer interface is placed) are notably greater than the ones at 40-mm depth. This effect does not happen for phantom 1 (one only layer) and the phantoms 4 and 5, for which the PVC powder brings a negligible impedance mismatch increase.

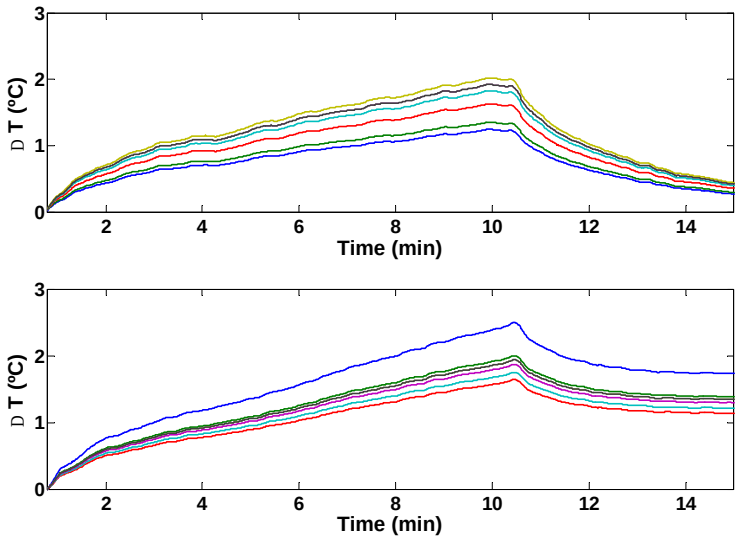

Figure 5. Temperature curves for phantom 5 (superior) and phantom 4 (inferior), insonified in continuous mode (2 W/cm^2) for 10 minutes.

The temperature increments for phantom 3 (0.6 g of graphite) are bigger than for phantom 2 (0.38 g of graphite). The only difference between these two phantoms is the powder quantity which modifies ϕ, and ℓ_S, but σ, μ and the external temperature are the same. We believe this increment can be attributed to two origins: one related to the absorption properties and the other related to the scattering which increases the US wave path. Therefore scattering has a double role. On one side it contributes to the global attenuation and, on the other side, generates more absorption as the mean freepath is bigger.

Table 3. Maximum temperature increases after a 10-minute insonification at 2.0 W/cm^2 for the five phantoms at seven depths. The interfaces of phantoms 2 to 5 are at 47 mm.

Depth	ΔTemperature (ºC)				
	Phantom				
	1	3	2	5	4
40 mm	1.41	1.18	1.18	1.95	1.95
45 mm	1.42	1.91	1.43	2.05	1.95
50 mm	1.34	2.92	1.48	1.95	1.88
55 mm	1.46	3.89	1.61	1.85	1.76
60 mm	1.41	4.23	1.56	1.65	1.65
75 mm	1.32	5.22	1.95	1.37	2.01
80 mm	1.27	5.41	2.31	1.26	2.51

In the same way, considering the phantom as isolated system for the duration of the experiments (no energy exchange with surroundings), the amount of energy (dQ) is proportional to the temperature increase (dT), that is the well known relation $dQ = mcdT$ (m is mass and c, the specific heat). For the same quantity of mass, temperature increment depends only on the medium specific heat. So, it should be expected that phantom 3 had twice the temperature increase than phantom 5 (Table 1). Indeed, the temperature increment is always more the

twice, as depicted in Table 3. A similar behaviour should then be expected to phantoms 2 and 4 that have (0.38g in powder), but, according to Table 3, they have similar ΔT. Thus, we believe it is a strong indication that scattering contributes to this phenomenon.

Another important aspect to consider is that, due to the presence of an interface in the two-layer phantoms, The US intensity transmitted to the second layer is dependent on the level of the acoustic impedance mismatch between both layers. For the phantoms in this work, the impedance for graphite is around 6.8 times the one for PVC, (Table 1), thus it is expected that less energy is transmitted to the second layer of the phantom 3, as compared to phantom 5. So as ΔT for the second layer in phantom 3 is always bigger, again scattering could be important to explain this behaviour.

CONCLUSIÓN

Some experimental results for the analysis of the influence of the ultrasonic scattering on tissue heating are presented. This experimental results show that, besides contributing for the global attenuation, scattering may play a non negligible role in the absorption of US energy once it promotes an increase in the mean free path for the US wave.
It is important to notice that it is usually assumed the Born approximation for US propagation in biological tissues. Nevertheless, it seems that this propagation regime should be reviewed as depth increases and tissue absorption (heating) is considered.
Further work is needed to analyse and model the contribution of ultrasonic scattering to tissue heating.

ACKNOWLEDGMENTS

For elaboration of this work the support of the CYTED/CNPq (PULSETS) project and ALPHA N I-0343-FA-FCD-FI (PETRA II) program has been received.

References: [1] Harvey E: Biological aspects of ultrasonic waves, a general survey. Biol Bull **59** (1930) 306-325
[2] Freundlich H, Söllner K, Rogowski F:. Einige biologische wirkungen von ultraschallwellen. Klin Wochschr 11 (1932) 1512-1513.
[3] Candi L. Garrett, David O., Draper, Kenneth L: Heat Distribution in the Lower Leg from Pulsed Short-Wave Diathermy and Ultrasound Treatments. Journal of Athletic Training **1, 35** (2000) 50-55
[4] Pennes H: Analysis of tissue and arterial temperatures in the resting human forearm. J. Appl. Physiol. **1,** (1948) 93-122.
[5] Ginter S.: Numerical simulation of ultrasound-thermotherapy combining nonlinear wave propagation with broadband soft-tissue absorption Ultrasonics 37 (2000) 693-696
[6] Gail ter Haar. Acoustic Surgery. Physics Today **54, 12 (**2001)
[7] Cortela G, Pereira, W, Negreira, C: Simulación del campo térmico generado por Transductores ultrasónicos circulares, In: IFMBE Proc. **5**, (2004) 1-4, João Pessoa,
[8] Meaney P., Cahill M.D., Ter Haar G: The intensity dependence of focused ultrasound lesion position, SPIE. **3249** (1998) 246-256.
[9] Filonenko E., Khokhlova V: Effect of acoustic nonlinearity on heating of biological tissue induced by high intensity focused ultrasound. Acoustical Physics.**47**, **4**, (2001) 541-549.
[10] Damianou C A, Sanghvin T, Fry. F, and Maass-Moreno. R: Dependence of ultrasonic attenuation and absorption in dog soft tissues on temperature and thermal dose. J. Acoustical Society of America, **102**, (1997) 628-34.
[11] Hynynen, K.: The role of nonlinear ultrasound propagation during hyperthermia treatments. Medical Physics. **18** (1991) 1156-1163
[12] Poan, Research Group, New Aspects of Electromagnetic and Acoustic Wave Diffusion, edited by G. Holer, Springer Tracts in Modern Physics, **144** Springer, Berlin, 1998.
[13] G. Bal and O. Pinaud: Accuracy of transport models for waves in random media. Wave Motion, **43**, (2006) 561–578
[14] A. Lagendikk et al: Resonant multiple scattering of light, Phys. Rep., **270**, (1996)
[15] D. Sornette: Acoustic waves in random media I. Weak disorder regime. Acustica, **67**, (1989) 199-215.
[16] Sheng, P: Introduction to Wave Scattering, Localization, and Mesoscopic Phenomena Academic, San Diego.